PLOS | ONE

RESEARCH ARTICLE

The Dynamic Conformational Cycle of the Group I Chaperonin C-Termini Revealed via Molecular Dynamics Simulation

Kevin M. Dalton[1], **Judith Frydman**[2], **Vijay S. Pande**[3]*

1 Biophysics Program, Stanford University, Stanford, California, United States of America, **2** Department of Biology, Stanford University, Stanford, California, United States of America, **3** Department of Chemistry, Stanford University, Stanford, California, United States of America

* pande@stanford.edu

Citation: Dalton KM, Frydman J, Pande VS (2015) The Dynamic Conformational Cycle of the Group I Chaperonin C-Termini Revealed via Molecular Dynamics Simulation. PLoS ONE 10(3): e0117724. doi:10.1371/journal.pone.0117724

Academic Editor: Vladimir N. Uversky, University of South Florida College of Medicine, UNITED STATES

Received: October 10, 2014

Accepted: December 31, 2014

Published: March 30, 2015

Data Availability Statement: Production trajectories, starting models, parameter file, and contact maps are available through the Stanford Digital Repository and can be accessed by the general public through the permanent URL: http://purl.stanford.edu/pn220pz6353.

Funding: This research was supported by the U.S. Department of Energy, Basic Energy Sciences, under grant DE-FG02-12ER16334 to JF and by the National Institutes of Health under grant 5R01GM062868-11 to VP. KD is supported by a Stanford Graduate Fellowship (http://sgf.stanford.edu/). The funders had no role in study design, data

Abstract

Chaperonins are large ring shaped oligomers that facilitate protein folding by encapsulation within a central cavity. All chaperonins possess flexible C-termini which protrude from the equatorial domain of each subunit into the central cavity. Biochemical evidence suggests that the termini play an important role in the allosteric regulation of the ATPase cycle, in substrate folding and in complex assembly and stability. Despite the tremendous wealth of structural data available for numerous orthologous chaperonins, little structural information is available regarding the residues within the C-terminus. Herein, molecular dynamics simulations are presented which localize the termini throughout the nucleotide cycle of the group I chaperonin, GroE, from Escherichia coli. The simulation results predict that the termini undergo a heretofore unappreciated conformational cycle which is coupled to the nucleotide state of the enzyme. As such, these results have profound implications for the mechanism by which GroE utilizes nucleotide and folds client proteins.

Introduction

Many cellular proteins cannot fold on their own and often become trapped in non-native intermediate conformations. Nature has evolved a variety of molecular chaperones that bind to and induce folding of these intermediates in an ATP dependent manner[1]. The chaperonins are one such class of molecular chaperone and are essential in nearly all characterized organisms. Chaperonins fold many different substrates and have been estimated to routinely interact with as much as 10% of the proteome[2–4].

The chaperonins are subdivided into two phyla, termed Group I and Group II chaperonins [5]. Group I chaperonins are found in prokaryotes as well as the eukaryotic organelles derived from endosymbiotic events, chloroplasts and mitochondria. The archetypal Group I chaperonin is the GroE system from *Escherichia coli*.

GroE consists of the GroEL complex, an $(\alpha_7)_2$ homoligomer with a dual-ring topology[6], and its homoheptameric cofactor, GroES, which acts as a lid for the GroEL folding chamber[7]

collection and analysis, decision to publish, or preparation of the manuscript.

Competing Interests: The authors have declared that no competing interests exist.

(Fig. 1A). GroEL monomers are 548 residues in length and have 3 domains (Fig. 1B). The equatorial domain is located at the ring interface and contains the ATP binding site[7,8]. The intermediate domain acts as a hinge upon which the apical domain pivots and contains the residues which form the apical surface of the nucleotide binding pocket (Fig. 1B). The apical domain binds to substrate proteins and to the GroES complex[8]. The apical domains of a given GroEL ring are competent to bind unfolded client proteins in the apo or ATP-bound configurations. Subsequent to substrate binding, GroES binding displaces the client protein in an ATP dependent manner, injecting it into the center of the chaperonin ring where it may fold in isolation. Substrate displacement is followed by nucleotide hydrolysis which is essential for GroES dissociation. GroES dissociation and substrate release complete the cycle.

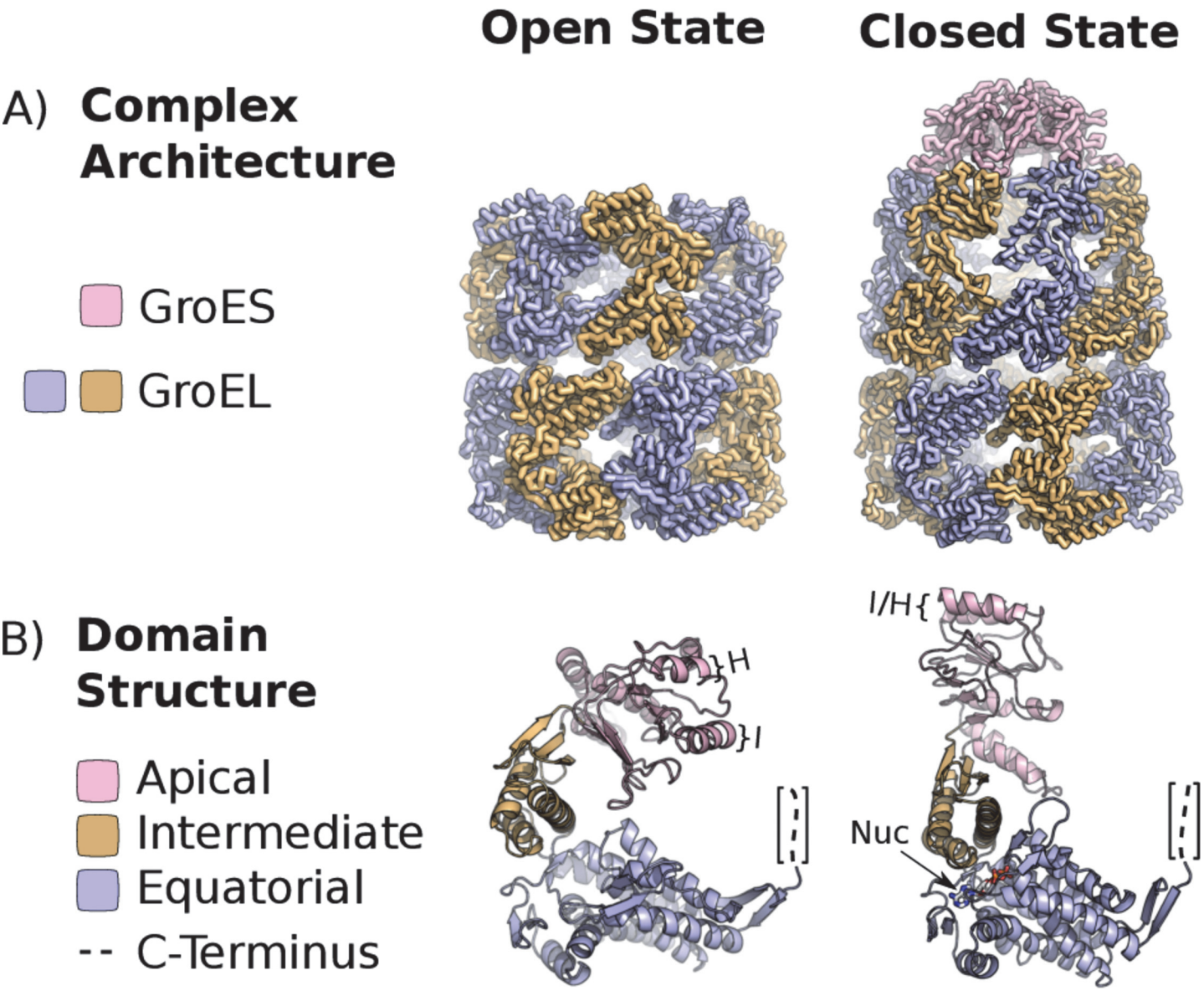

Fig 1. The Molecular Architecture of GroE. The crystal structure of the GroE chaperonin from Escherichia coli in the open, ATP-bound (PDBID: 1KP8) and closed (PDBID: 1AON) states. The full complex and single subunits are depicted in panels A and B respectively. Helices I and H as well as the nucleotide binding pocket are indicated in B. Structures were rendered in PyMOL.

doi:10.1371/journal.pone.0117724.g001

Substrate encapsulation is the hallmark of the chaperonin nucleotide cycle which differentiates it from other molecular chaperones[1]. Encapsulation is essential for efficient folding of substrates. There are many proposed mechanisms by which encapsulation improves folding yields[9]. The most obvious mechanism is the prevention of intermolecular aggregation by isolating the substrate from the cellular protein pool which may be the chaperonin's lone mechanism for a portion of its substrates[10]. Nonetheless, it has been demonstrated that the microenvironment of the GroE cavity accelerates the folding of other substrates yielding faster folding rates than are observed for the same protein in free solution[11]. This rate enhancement appears to originate from a variety of sources. Chief among these is the steric exclusion of extended conformers in the unfolded ensemble[12,13], modulation of the solvent environment by the cavity walls[14–16] and an unfolding event early in the encapsulation process[17]. The mechanism by which the three major structural domains of GroEL function together to give rise to this closed, encapsulated state is well understood.

In addition to the three well characterized domains, GroEL possesses a C-terminal region which is a disordered segment of 23 amino acids following Pro-525. A short hydrophilic motif, P525—KNDAAD—L532, followed by an approximate repeat of the Gly-Gly-Met tripeptide comprise this terminal segment. Numerous structures of chaperonins containing terminal repeats have been solved representing both the open and closed configurations[6,7,18–27]. Despite the high resolution of these structures, the C-termini do not appear in the electron density maps indicating that they exist in an ensemble of conformations. In archaeal Group II chaperonins, the role of the disordered C-termini is clear in that they determine the thermostability of the complex [28]. By contrast, deletion of the disordered region at the C-terminus of GroEL does not seem to perturb the stability of the complex or demonstrate a growth defect in vivo[29]. Consequently, the role of the GroEL C-termini in the chaperonin mechanism is rather subtle. Deletion of the C-terminal repeats in GroEL modestly decreases both the ATPase rate[30,31] and the folding activity[32] of the enzyme. Furthermore, disulfide crosslinking of substrates to GroEL demonstrated that the repeats are in close proximity to bound substrate prior to encapsulation[33]. The interaction of bound substrates with the C-terminus demonstrated by in vitro crosslinking[33] has been corroborated by a proteomic study which demonstrated differential substrate specificity for two variants of GroEL with different C-terminal sequences[34]. Taken together these results indicate that the GGM repeats play a role in substrate recognition. More recent work supports the hypothesis that the C-termini of GroEL are involved in substrate encapsulation in addition to binding Specifically, this work demonstrated that the C-termini interact with the substrate protein RuBisCO during the encapsulation process, enhance the yield of substrate encapsulation[35], and remodel the substrate's conformation before and throughout encapsulation[17].

Despite this sizable body of biochemical work, it is still unclear how the termini fit into the overall structural mechanism of GroE. Why does their deletion perturb the ATPase and folding rates of the enzyme?

Results

In order to elucidate the mechanism by which the C-terminus influences the activity of GroEL, we sought structural information about the GGM repeats via molecular dynamics simulations. In this study, the open, ATP-bound (PDB ID: 1KP8)[36] and closed ADP-bound (PDB ID: 1AON)[7] structures of GroE were simulated in implicit solvent for a total of 190 ns each. In order to limit the computational complexity of the simulations, the N-terminal 523 amino acids of GroEL as well as all the residues of GroES were frozen throughout the simulations. The two simulations contained three distinct types of chaperonin rings corresponding to three intermediates of the GroE nucleotide cycle. Both rings of the open state simulation, based on

PDBID: 1KP8, correspond to an ATP bound ring which is competent to bind unfolded substrates. The closed state simulation based on PDBID: 1AON contained two types of chaperonin rings. In particular, the trans-ring corresponds to an apo ring lacking any bound nucleotide which is also competent to bind substrate. By contrast, the cis-ring of the same simulation is bound by GroES as well as ADP. The cis-ring has thereby formed a folding chamber in which substrates may be encapsulated. The three ring types will be referred to as the holo for ATP-bound, apo for the trans-ring of the closed state simulation, and closed for the GroES-bound ring. It is pertinent to note that the holo and apo rings have very similar conformations exhibiting a 1.4 Å RMSD (S4 Fig.).

Analysis of the GroE Langevin dynamics simulations yielded very similar C-terminal conformations between the apo and holo rings. However, the conformation of the termini differed markedly for the closed ring. In order to represent the difference in conformation between the states of GroE, contact maps were constructed with g_mdmat from Gromacs[37] (S1, S2 Figs.). The C-terminal 23 amino acids which form the GGM repeats were then investigated in the context of these contact maps (Fig. 2). The conformation of these residues differs strikingly between closed ring and two rings not bound by GroES. In both simulations, the repeats showed the strongest contact with other residues within the termini (Fig. 2 B,E,H red) which is unsurprising given the proximity between these residues in the primary sequence. Nonetheless, the apo and holo rings' termini showed considerable interaction with residues within the apical domain of the chaperonin (Fig. 2 B,E pink). The most significant interactions are between the terminus and hydrophobic residues lining the inner face of the apical domain's helix I (Fig. 1C) which has been implicated in substrate binding by biochemical and structural studies. Particularly strong interactions are observed for residues R268, M267, V263 & L259 (Fig. 2 C,F). Notably, these hydrophobic residues are thought to directly contact the substrate, and mutations at V263 and L259 have been shown to perturb the binding of both substrate and GroES to GroEL [8]. The validity of the apo and holo ring ensembles is bolstered by a recent cryoelectron microscopy study[35] which demonstrated complex electron density in the trans-ring of the singly-closed GroEL/ES. The authors of this study speculated that the trans-ring density may originate from extended C-termini. By contrast, in the closed state, helix I of the apical domain is retracted upward and is occupied by GroES. Hence, the C-termini no longer contact the apical domain of the active folding chamber and only interact weakly with residues outside of the flexible tail. These interactions are predominantly restricted to the stem loop of the equatorial domain (Fig. 2 I), which is proximal to the nucleotide binding site.

Discussion

The simulations presented herein predict a new conformational cycle within the group I chaperonin which has proven inaccessible to classical structural biology. The cycle, schematized in Fig. 3, summarizes the manner in which the GroE ATPase cycle impacts the structure of the C-termini and how the termini alter the chemical environment within the cavity throughout. This work provides a plausible conformational ensemble for the C-termini of ATP-bound rings, apo trans-rings and of ADP-bound cis-rings. No attempt has been made to extensively model the intermediate conformations in this cycle owing to a lack of atomic level structural data on these states. C-terminal conformations indicated by dashed lines in Fig. 3 are at present hypothetical and not contained within the simulation data. In the context of this model, it is possible to reconcile a portion of the biochemical data regarding the chaperonin C-termini.

Irrespective of the particular structural mechanism, the simulations predict that the conformation of the C-termini must transition along the pathway between the apo and closed, cis-ring conformations. While the precise details of when or how these transitions occur are yet to be

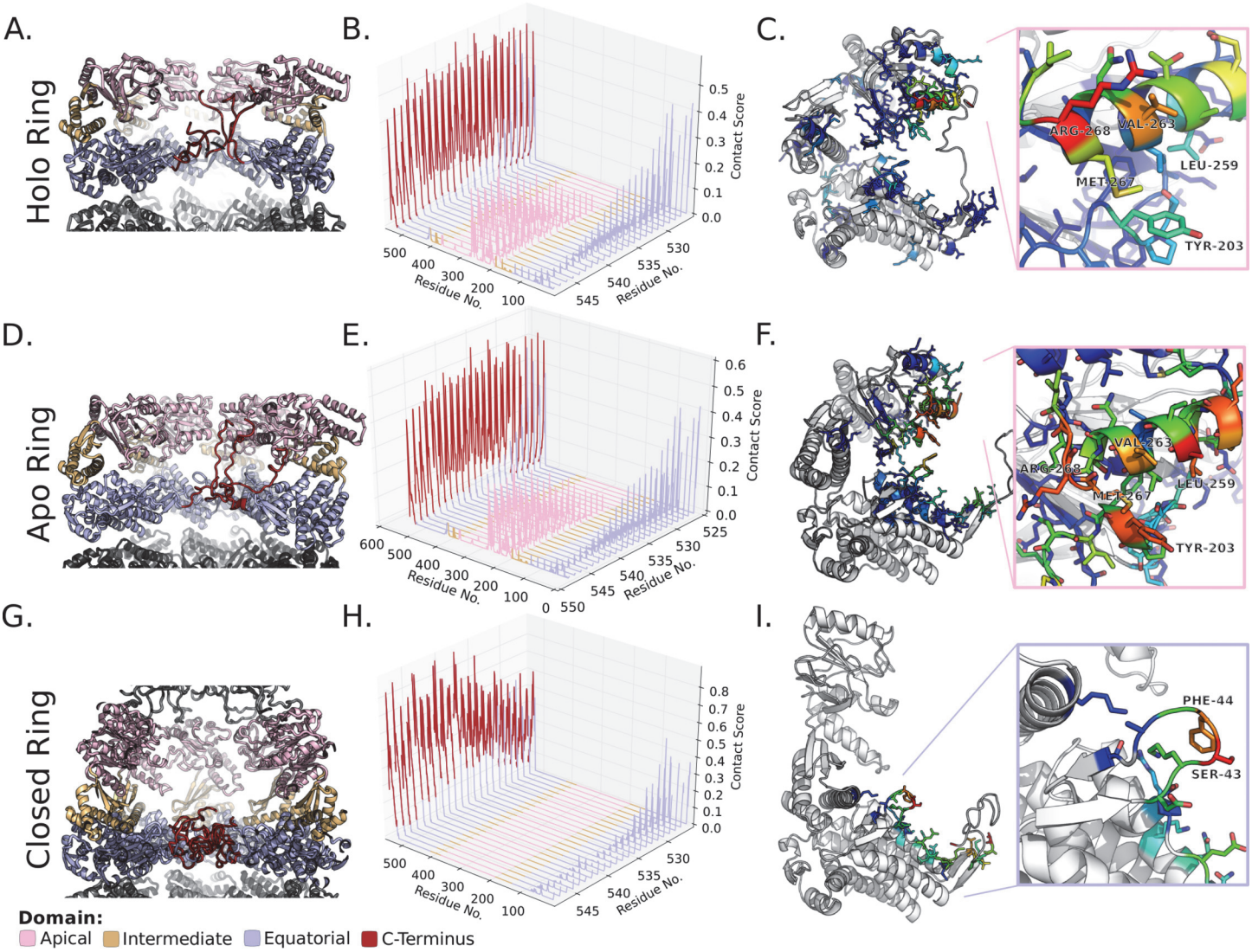

Fig 2. Characterization of C-terminal Contacts in GroE Simulations. Residue contacts of the GroEL C-terminus from 190 ns of implicit solvent molecular dynamics simulations. A,D,G) Representative snapshots of the the GroE simulations colored by domain as indicated. B,E,H) Residue contacts between the terminal residues and the rest of the chaperonin residues from the open and closed state simulations. Higher values represent more frequent contacts. C,F,I) Heat maps of the terminal residue's (M548) contacts mapped onto representative monomer from the simulations. The monomer structures derive from the holo enzyme simulation (C), the trans-ring of the GroES bound (F), and the cis-ring of the GroES bound (I) simulations. The insets represent helix I (C,F) or the stem loop (I). C) A heat map of the holo ring's M548 contacts mapped onto a representative snapshot from the simulation. Inset: view of the apical domain helix I colored by M548 contact frequency. In panels C, F, & I contacts between M548 and other tail residues have been omitted by setting their values as zero. Structures were rendered in PyMOL.

doi:10.1371/journal.pone.0117724.g002

determined, the termini must necessarilly be involved in the transition states of the opening and closing conformational changes. It should thus be expected that their deletion would effect the energy of the transition states. Thereby, the deletion of the termini should influence the closing and opening rates of GroE. The involvement of the termini in the transition between the open and closed conformations clarifies why deletion of the termini influences the ATPase rate of the enzyme[30,31].

In addition to the termini's involvement in the nucleotide cycle, the simulations predict that the C-termini play a role in substrate binding. It has already been shown that the C-termini of GroEL engage the substrate upon binding and that they are structurally and biochemically

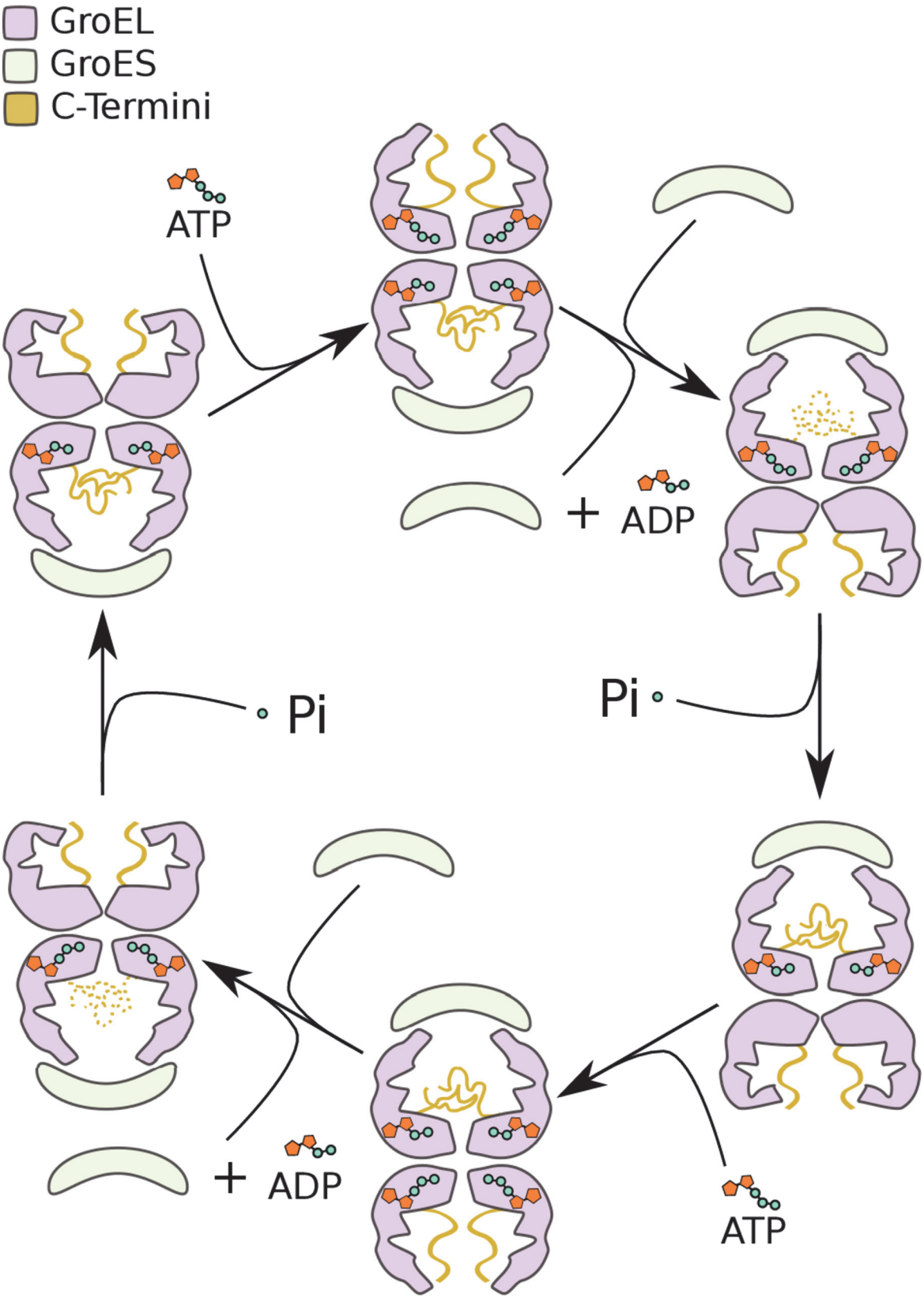
GroEL
GroES
C-Termini
ATP
+ ADP
Pi
Pi
+ ADP
ATP

Fig 3. The Dynamic Conformational Cycle of the GroEL C-Termini. Schematic representation of the GroE nucleotide cycle emphasizing the C-terminal conformational dynamics/cycle. The conformational cycle of the C-terminal tails is indicated throughout the group I chaperonin nucleotide cycle. States with the C-termini rendered as dashes are hypothetical while those rendered with solid lines represent rings contained in our simulations.

doi:10.1371/journal.pone.0117724.g003

involved in the encapsulation process[35,17]. However, the concentration of the C-termini at helix I (Fig. 2 C,F) in the apo and holo rings, predicts that the GGM repeats may occupy the substrate binding site prior to substrate binding. The apical localization of the termini therefore has implications for the manner in which GroE recognizes substrates. As they occupy the binding site, the GGM repeats must modulate the affinity of the GroEL apical domains for clients. Biochemical evidence[35] indicates that the C-terminus of GroEL contributes to the effective encapsulation of substrates. This suggests that the GGM repeats increase the affinity of the chaperonin for unfolded clients in the apo state as well as the intermediate states leading to closure of the folding chamber. Based on the apo state conformational ensemble, the termini likely increase the affinity by providing a secondary substrate binding site. It is tempting to speculate that this secondary binding site may possess broader specificity than the apical domain Helix I owing to its low sequence complexity and lack of secondary structure. Consequently the GGM repeats may ensure that the chaperonin interacts with a broader range of misfolded clients than may otherwise be possible. The precedent for modulation of the chaperonin substrate pool by the termini has been demonstrated proteomically[34] indicating that substrate binding is one important function of the GGM repeats.

The isolation of the termini at the bottom of the folding chamber in the closed state does not portend an active role for the termini in the foldase activity[11] of the GroE cavity. However, these simulations were carried out in the absence of substrate, and it is impossible to know precisely how an encapsulated substrate may alter the conformational ensemble of the C-termini. Nevertheless, it has been demonstrated that the deletion of the GroEL C-termini alters the folding trajectory of RuBisCO[17]. Therefore it is clear that the C-termini can influence substrate conformation potentially by steric interaction or alternatively by altering the electrostatic environment of the folding chamber. The generality as well as the precise mechanism by which substrate folding trajectories can be modulated remains to be assessed. Nonetheless, this work dictates a clear role for the termini in engaging the manifold chaperonin substrates within the crowded cellular millieu.

Materials and Methods

The open, ATP-bound (PDB ID: 1KP8)[36] and closed ADP-bound (PDB ID: 1AON)[7] structures of GroE were simulated in implicit solvent for a total of 190 ns each. The C-terminal 23 residues were modeled into the crystal structures by hand in COOT[38]. The N-terminal methionine was not reintroduced into the structures as there was no density for it in the crystallographic electron density maps and the N-terminal methionine is often cleaved nascently by *Escherichia coli* methionine aminopeptidase. As a result, the GroEL models used here contain 547 amino acid residues per monomer. Nucleotide atoms were omitted from the simulations. However, the conformation of the atoms lining the nucleotide binding pocket were preserved as described below.

The structures were protonated and energy minimized in Gromacs[37]. Subsequently, the N-terminal 523 residues were defined as a freeze group and were fixed in space to reduce the complexity of the simulations. The two energy minimized structures were simulated in five 10 ns simulations per conformation in GBSA[39] implicit solvent and thermostatted via velocity rescaling at 370K. These simulations were subsampled to generate 19 starting conformers for each system. The starting conformations were subjected to 10 ns Langevin dynamics

simulations at 370K yielding a total of 190 ns of data for each GroE conformer. The combination of high temperature with the GBSA solvation model has been shown to be predictive of protein dynamics[40,41]. All analyses presented here originate from the Langevin simulations. All simulations utilized the Amber99SB-ILDN forcefield[42]. Additional data analysis methods can be found in the supporting information. Supplemental movies were rendered in VMD[43].

Supporting Information

S1 File. Calculation of Unsymmetrized Contact Maps. Description of the calculation of the symmetrized contact maps discussed in this manuscript.
(PDF)

S1 Fig. Unsymmetrized Contact Maps. The raw per-residue contact maps calculated with g_mdmat. Contact maps were calculated for each of the 38 10 ns simulations. The 19 maps corresponding to each conformation of GroE were summed to yield the maps here. Maps were normalized by dividing by the maximum value in the matrix. The open state simulation was based on PDBID:1KP8 while the closed state simulation was based on PDBID:1AON.
(TIFF)

S2 Fig. Tiling of Unsymmetrized Contact Map. Tiling of the open state contact map presented in S1. Each box represents the interaction between GroEL monomer i and j within the holo complex simulation. The symmetrized contact maps in S3 were generated by summing these boxes.
(TIFF)

S3 Fig. Symmetrized Contact Maps. Symmetrized maps for the open and closed state simulations of GroE. The open state was constructed from the sum of all the 547X547 blocks in the unsymmetrized map. The closed state map only reflects interactions between monomers of the cis-ring in the closed state simulation.
(TIF)

S4 Fig. Comparison of Trans-apo and ATP Bound Monomers. 3D alignment of a monomer from the trans-ring of PDBID: 1AON with a monomer from the ATP-bound structure, PDBID: 1KP8. The all atom RMSD between the structures is 1.4Å. The structural alignment was generated and rendered using the PyMOL molecular graphics software.
(TIF)

S1 Movie. GroEL ATP-Bound Simulation. Movie depicting twenty concatenated 10 ns simulations of a GroEL holo ring (based on PDBID: 1KP8). Residues rendered in blue were frozen throughout the course of the simulation. Orange residues are in the C-terminal region and these were allowed to move in time.
(MPG)

S2 Movie. GroE Cis-Ring Simulation. Movie depicting twenty concatenated 10 ns simulations of the GroEL/ES complex (based on PDBID: 1AON). Residues rendered in blue were frozen throughout the course of the simulation. Orange residues are in the C-terminal region and these were allowed to move in time. The rendering is focused on the folding chamber referred to as the cis-ring.
(MPG)

S3 Movie. GroE Trans-Ring Simulation. Movie depicting twenty concatenated 10 ns simulations of GroEL/ES in the closed state (based on PDBID: 1AON). Residues rendered in blue were frozen throughout the course of the simulation. Orange residues are in the C-terminal

region and these were allowed to move in time. The rendering is focused on the trans-ring, which is in the apo configuration.
(MPG)

Acknowledgments

The authors would like to acknowledge the excellent Python language graphics toolkit, Matplotlib used to generate the plots in this work[44]. The authors would also like to acknowledge the NumPy, SciPy, and IPython[45,46] projects which were instrumental for data reduction and analysis.

Author Contributions

Conceived and designed the experiments: KMD VSP. Performed the experiments: KMD. Analyzed the data: KMD. Contributed reagents/materials/analysis tools: KMD JF VSP. Wrote the paper: KMD JF VSP.

References

1. Hartl FU, Bracher A, Hayer-Hartl M (2011) Molecular chaperones in protein folding and proteostasis. Nature 475: 324–332. Available: http://www.ncbi.nlm.nih.gov/pubmed/21776078. Accessed 26 October 2012. doi: 10.1038/nature10317 PMID: 21776078
2. Kerner MJ, Naylor DJ, Ishihama Y, Maier T, Chang H-C, et al. (2005) Proteome-wide analysis of chaperonin-dependent protein folding in Escherichia coli. Cell 122: 209–220. Available: http://www.ncbi.nlm.nih.gov/pubmed/16051146. Accessed 7 August 2013. PMID: 16051146
3. Houry W, Frishman D, Eckerskorn C (1999) Identification of in vivo substrates of the chaperonin GroEL. Nature: 147–154. Available: http://www.cs.huji.ac.il/csls2000/studies/compubio/Tamar_578D5A74d01.ps. Accessed 7 December 2012. PMID: 10647006
4. Gong Y, Kakihara Y, Krogan N, Greenblatt J, Emili A, et al. (2009) An atlas of chaperone-protein interactions in Saccharomyces cerevisiae: implications to protein folding pathways in the cell. Mol Syst Biol 5: 275. Available: http://www.pubmedcentral.nih.gov/articlerender.fcgi?artid=2710862&tool = pmcentrez&rendertype = abstract. Accessed 7 March 2013. doi: 10.1038/msb.2009.26 PMID: 19536198
5. Horwich AL, Fenton W a, Chapman E, Farr GW (2007) Two families of chaperonin: physiology and mechanism. Annu Rev Cell Dev Biol 23: 115–145. Available: http://www.ncbi.nlm.nih.gov/pubmed/17489689. Accessed 12 March 2013. PMID: 17489689
6. Braig K, Otwinowski Z, Hegde R, Boisvert DC, Joachimiak A, et al. (1994) The crystal structure of the bacterial chaperonin GroEL at 2.8 A. Nature 371: 578–586. Available: http://www.nature.com/nsmb/journal/v3/n2/abs/nsb0296-170.html. PMID: 7935790
7. Xu Z, Horwich a L, Sigler PB (1997) The crystal structure of the asymmetric GroEL-GroES-(ADP)7 chaperonin complex. Nature 388: 741–750. Available: http://www.ncbi.nlm.nih.gov/pubmed/9285585. PMID: 9285585
8. Fenton W, Kashi Y, Furtak K, Horwich A (1994) Residues in chaperonin GroEL required for polypeptide binding and release. Nature 371: 614–619. Available: http://www.nature.com/nature/journal/v371/n6498/abs/371614a0.html. Accessed 7 December 2012. PMID: 7935796
9. Lucent D, England J, Pande V (2009) Inside the chaperonin toolbox: theoretical and computational models for chaperonin mechanism. Phys Biol 6: 015003. Available: http://www.ncbi.nlm.nih.gov/pubmed/19208937. Accessed 12 July 2011. doi: 10.1088/1478-3975/6/1/015003 PMID: 19208937
10. Tyagi NK, Fenton W a, Deniz A a, Horwich AL (2011) Double mutant MBP refolds at same rate in free solution as inside the GroEL/GroES chaperonin chamber when aggregation in free solution is prevented. FEBS Lett 585: 1969–1972. Available: http://www.pubmedcentral.nih.gov/articlerender.fcgi?artid=3144026&tool = pmcentrez&rendertype = abstract. doi: 10.1016/j.febslet.2011.05.031 PMID: 21609718
11. Brinker a, Pfeifer G, Kerner MJ, Naylor DJ, Hartl FU, et al. (2001) Dual function of protein confinement in chaperonin-assisted protein folding. Cell 107: 223–233. Available: http://www.ncbi.nlm.nih.gov/pubmed/11672529. PMID: 11672529
12. Zhou H, Dill KA (2001) New Concepts Stabilization of Proteins in Confined Spaces †. Biochemistry 40: 11289–11293. Available: http://pubs.acs.org/doi/abs/10.1021/bi0155504. PMID: 11560476

13. Hofmann H, Hillger F, Pfeil SH, Hoffmann A, Streich D, et al. (2010) Single-molecule spectroscopy of protein folding in a chaperonin cage. Proc Natl Acad Sci U S A 107: 11793–11798. Available: http://www.pubmedcentral.nih.gov/articlerender.fcgi?artid=2900638&tool = pmcentrez&rendertype = abstract. Accessed 22 July 2011. doi: 10.1073/pnas.1002356107 PMID: 20547872

14. Lucent D, Vishal V, Pande VS (2007) Protein folding under confinement: a role for solvent. Proc Natl Acad Sci U S A 104: 10430–10434. Available: http://www.pubmedcentral.nih.gov/articlerender.fcgi?artid=1965530&tool = pmcentrez&rendertype = abstract. PMID: 17563390

15. England J, Lucent D, Pande V (2008) A role for confined water in chaperonin function. J Am . . .: 11838–11839. Available: http://pubs.acs.org/doi/abs/10.1021/ja802248m. Accessed 2 November 2012.

16. Weber JK, Pande VS (2013) Functional understanding of solvent structure in GroEL cavity through dipole field analysis. J Chem Phys 138: 165101. Available: http://www.ncbi.nlm.nih.gov/pubmed/23635172. Accessed 8 May 2013. doi: 10.1063/1.4801942 PMID: 23635172

17. Weaver J, Rye HS (2014) The C-terminal tails of the bacterial chaperonin GroEL stimulate protein folding by directly altering the conformation of a substrate protein. J Biol Chem 289: 23219–23232. Available: http://www.ncbi.nlm.nih.gov/pubmed/24970895. Accessed 11 December 2014. doi: 10.1074/jbc.M114.577205 PMID: 24970895

18. Shomura Y, Yoshida T, Iizuka R, Maruyama T, Yohda M, et al. (2004) Crystal Structures of the Group II Chaperonin from Thermococcus strain KS-1: Steric Hindrance by the Substituted Amino Acid, and Inter-subunit Rearrangement between Two Crystal Forms. J Mol Biol 335: 1265–1278. Available: http://linkinghub.elsevier.com/retrieve/pii/S0022283603014062. Accessed 2 November 2012. PMID: 14729342

19. Pereira JH, Ralston CY, Douglas NR, Meyer D, Knee KM, et al. (2010) Crystal structures of a group II chaperonin reveal the open and closed states associated with the protein folding cycle. J Biol Chem 285: 27958–27966. Available: http://www.pubmedcentral.nih.gov/articlerender.fcgi?artid=2934662&tool = pmcentrez&rendertype = abstract. Accessed 12 July 2011. doi: 10.1074/jbc.M110.125344 PMID: 20573955

20. Ditzel L, Löwe J, Stock D, Stetter KO, Huber H, et al. (1998) Crystal structure of the thermosome, the archaeal chaperonin and homolog of CCT. Cell 93: 125–138. Available: http://www.ncbi.nlm.nih.gov/pubmed/9546398. PMID: 9546398

21. Dekker C, Roe SM, McCormack EA, Beuron F, Pearl LH, et al. (2011) The crystal structure of yeast CCT reveals intrinsic asymmetry of eukaryotic cytosolic chaperonins. EMBO J 30: 3078–3090. Available: http://www.pubmedcentral.nih.gov/articlerender.fcgi?artid=3160183&tool = pmcentrez&rendertype = abstract. Accessed 29 October 2012. doi: 10.1038/emboj.2011.208 PMID: 21701561

22. Leitner A, Joachimiak LA, Bracher A, Mönkemeyer L, Walzthoeni T, et al. (2012) The molecular architecture of the eukaryotic chaperonin TRiC/CCT. Structure 20: 814–825. Available: http://www.ncbi.nlm.nih.gov/pubmed/22503819. Accessed 2 November 2012. doi: 10.1016/j.str.2012.03.007 PMID: 22503819

23. Ranson N a, Farr GW, Roseman a M, Gowen B, Fenton W a, et al. (2001) ATP-bound states of GroEL captured by cryo-electron microscopy. Cell 107: 869–879. Available: http://www.ncbi.nlm.nih.gov/pubmed/11779463. PMID: 11779463

24. Clare DK, Vasishtan D, Stagg S, Quispe J, Farr GW, et al. (2012) ATP-triggered conformational changes delineate substrate-binding and -folding mechanics of the GroEL chaperonin. Cell 149: 113–123. Available: http://www.pubmedcentral.nih.gov/articlerender.fcgi?artid=3326522&tool = pmcentrez&rendertype = abstract. Accessed 2 November 2012. doi: 10.1016/j.cell.2012.02.047 PMID: 22445172

25. Zhang J, Baker ML, Schröder GF, Douglas NR, Reissmann S, et al. (2010) Mechanism of folding chamber closure in a group II chaperonin. Nature 463: 379–383. Available: http://www.pubmedcentral.nih.gov/articlerender.fcgi?artid=2834796&tool = pmcentrez&rendertype = abstract. Accessed 12 July 2011. doi: 10.1038/nature08701 PMID: 20090755

26. Douglas NR, Reissmann S, Zhang J, Chen B, Jakana J, et al. (2011) Dual action of ATP hydrolysis couples lid closure to substrate release into the group II chaperonin chamber. Cell 144: 240–252. Available: http://www.pubmedcentral.nih.gov/articlerender.fcgi?artid=3055171&tool = pmcentrez&rendertype = abstract. Accessed 2 November 2012. doi: 10.1016/j.cell.2010.12.017 PMID: 21241893

27. Cong Y, Schröder GF, Meyer AS, Jakana J, Ma B, et al. (2012) Symmetry-free cryo-EM structures of the chaperonin TRiC along its ATPase-driven conformational cycle. EMBO J 31: 720–730. Available: http://www.pubmedcentral.nih.gov/articlerender.fcgi?artid=3273382&tool = pmcentrez&rendertype = abstract. Accessed 2 November 2012. doi: 10.1038/emboj.2011.366 PMID: 22045336

28. Luo H, Robb FT (2011) A modulator domain controlling thermal stability in the Group II chaperonins of Archaea. Arch Biochem Biophys 512: 111–118. Available: http://www.ncbi.nlm.nih.gov/pubmed/21600187. Accessed 31 October 2011. doi: 10.1016/j.abb.2011.04.017 PMID: 21600187

29. Burnett BP, Horwich AL, Low KB (1994) A carboxy-terminal deletion impairs the assembly of GroEL and confers a pleiotropic phenotype in Escherichia coli K-12. J Bacteriol 176: 6980–6985. Available: http://www.pubmedcentral.nih.gov/articlerender.fcgi?artid=197070&tool = pmcentrez&rendertype = abstract. PMID: 7961461

30. Farr GW, Fenton W a, Horwich AL (2007) Perturbed ATPase activity and not "close confinement" of substrate in the cis cavity affects rates of folding by tail-multiplied GroEL. Proc Natl Acad Sci U S A 104: 5342–5347. Available: http://www.pubmedcentral.nih.gov/articlerender.fcgi?artid=1828711&tool = pmcentrez&rendertype = abstract. Accessed 2 November 2012. PMID: 17372195

31. Machida K, Kono-Okada A, Hongo K, Mizobata T, Kawata Y (2008) Hydrophilic residues 526 KNDAAD 531 in the flexible C-terminal region of the chaperonin GroEL are critical for substrate protein folding within the central cavity. J Biol Chem 283: 6886–6896. Available: http://www.ncbi.nlm.nih.gov/pubmed/18184659. Accessed 8 May 2013. doi: 10.1074/jbc.M708002200 PMID: 18184659

32. Tang Y-C, Chang H-C, Roeben A, Wischnewski D, Wischnewski N, et al. (2006) Structural features of the GroEL-GroES nano-cage required for rapid folding of encapsulated protein. Cell 125: 903–914. Available: http://www.ncbi.nlm.nih.gov/pubmed/16751100. Accessed 12 July 2011. PMID: 16751100

33. Elad N, Farr GW, Clare DK, Orlova E V, Horwich AL, et al. (2007) Topologies of a substrate protein bound to the chaperonin GroEL. Mol Cell 26: 415–426. Available: http://www.pubmedcentral.nih.gov/articlerender.fcgi?artid=1885994&tool = pmcentrez&rendertype = abstract. Accessed 7 December 2012. PMID: 17499047

34. Wang Y, Zhang W, Zhang Z, Li J, Li Z, et al. (2013) Mechanisms involved in the functional divergence of duplicated GroEL chaperonins in Myxococcus xanthus DK1622. PLoS Genet 9: e1003306. Available: http://www.pubmedcentral.nih.gov/articlerender.fcgi?artid=3578752&tool = pmcentrez&rendertype = abstract. Accessed 3 May 2013. doi: 10.1371/journal.pgen.1003306 PMID: 23437010

35. Chen D-H, Madan D, Weaver J, Lin Z, Schröder GF, et al. (2013) Visualizing GroEL/ES in the Act of Encapsulating a Folding Protein. Cell 153: 1354–1365. Available: http://linkinghub.elsevier.com/retrieve/pii/S009286741300528X. Accessed 7 June 2013. doi: 10.1016/j.cell.2013.04.052 PMID: 23746846

36. Wang J, Boisvert DC (2003) Structural Basis for GroEL-assisted Protein Folding from the Crystal Structure of (GroEL-KMgATP)14 at 2.0Å Resolution. J Mol Biol 327: 843–855. Available: http://linkinghub.elsevier.com/retrieve/pii/S0022283603001840. Accessed 3 October 2013. PMID: 12654267

37. Hess B, Uppsala S-, Lindahl E (2008) GROMACS 4: Algorithms for Highly Efficient, Load-Balanced, and Scalable Molecular Simulation: 435–447.

38. Emsley P, Lohkamp B, Scott WG, Cowtan K (2010) Features and development of Coot. Acta Crystallogr D Biol Crystallogr 66: 486–501. Available: http://www.pubmedcentral.nih.gov/articlerender.fcgi?artid=2852313&tool = pmcentrez&rendertype = abstract. Accessed 4 March 2013. doi: 10.1107/S0907444910007493 PMID: 20383002

39. Still W, Tempczyk A (1990) Semianalytical treatment of solvation for molecular mechanics and dynamics. J . . .: 6127–6129. Available: http://pubs.acs.org/doi/abs/10.1021/ja00172a038. Accessed 3 May 2013.

40. Voelz V a, Jäger M, Yao S, Chen Y, Zhu L, et al. (2012) Slow unfolded-state structuring in Acyl-CoA binding protein folding revealed by simulation and experiment. J Am Chem Soc 134: 12565–12577. Available: http://www.ncbi.nlm.nih.gov/pubmed/22747188. doi: 10.1021/ja302528z PMID: 22747188

41. Voelz V a, Bowman GR, Beauchamp K, Pande VS (2010) Molecular simulation of ab initio protein folding for a millisecond folder NTL9(1–39). J Am Chem Soc 132: 1526–1528. Available: http://www.pubmedcentral.nih.gov/articlerender.fcgi?artid=2835335&tool = pmcentrez&rendertype = abstract. doi: 10.1021/ja9090353 PMID: 20070076

42. Lindorff-Larsen K, Piana S, Palmo K, Maragakis P, Klepeis JL, et al. (2010) Improved side-chain torsion potentials for the Amber ff99SB protein force field. Proteins 78: 1950–1958. Available: http://www.pubmedcentral.nih.gov/articlerender.fcgi?artid=2970904&tool = pmcentrez&rendertype = abstract. Accessed 6 August 2013. doi: 10.1002/prot.22711 PMID: 20408171

43. Humphrey W, Dalke a, Schulten K (1996) VMD: visual molecular dynamics. J Mol Graph 14: 33–38, 27–28. Available: http://www.ncbi.nlm.nih.gov/pubmed/8744570. PMID: 8744570

44. Hunter JD (2007) Matplotlib: A 2D graphic environment. Comput Sci Eng 9: 90–95. Available: http://ieeexplore.ieee.org/xpl/abstractKeywords.jsp?arnumber=4160265.

45. Oliphant TE (2007) Python for Scientific Computing. Comput Sci Eng 9: 10–20. Available: http://ieeexplore.ieee.org/lpdocs/epic03/wrapper.htm?arnumber=4160250.

46. Pérez F, Granger BE (2007) IPython: A System for Interactive Scientific Computing. Comput Sci Eng 9: 21–29. Available: http://ieeexplore.ieee.org/xpl/articleDetails.jsp?arnumber=4160251.